Supporting Information

Oriented Porous NASICON 3D Framework via Freeze Casting for Sodium Metal Batteries

Eldho Edison[1], Annapaola Parrilli[2], Elena Tervoort[1], Henrik Eliasson[3], Markus Niederberger[1]*

[1]Laboratory for Multifunctional Materials, Department of Materials, ETH Zürich, Vladimir-Prelog-Weg 5, Zurich, 8093, Switzerland

[2]Center for X-Ray Analytics, Empa - Swiss Federal Laboratories for Materials Science & Technology, Dübendorf, 8600 Switzerland

[3]Electron Microscopy Center, Empa - Swiss Federal Laboratories for Materials Science & Technology, Dübendorf, 8600, Switzerland

[*]E-mail: eedison@ethz.ch (E. Edison)

Experimental Methods

Materials: Sodium aluminum titanium phosphate ($Na_{1.3}Al_{0.3}Ti_{1.7}P_3O_{12,}$ NATP) was purchased from NEI Corporation, USA (NANOMYTE® NAB-1000). All chemicals were used as received without any further purification. Polyvinyl alcohol (PVA, MW=9000-1000, Sigma Aldrich). Polyethylene glycol (PEG, MW=200, Sigma Aldrich). Vanadium pentoxid**e** (>=99.6%, Sigma Aldrich, 221899-250G). Ammonium dihydrogen phosphate (99.999% trace metal basis, Sigma Aldrich 204005). Sodium carbonate (>99.9%, MERCK). Ascorbic acid (99%, Sigma Aldrich). Carbon black (Imerys Graphite & Carbon, Super C65). Polyvinylidene fluoride (PVDF, average Mw ~534,000, Sigma Aldrich 182702-100G). *N*-methyl-2-pyrrolidone (99.5%, Thermo Scientific-Acros Organics). Sodium perchlorate anhydrous (>98%, Alfa Aesar 011623-22). Propylene carbonate anhydrous (99.7%, Sigma Aldrich). Fluoroethylene carbonate (99%, Sigma Aldrich). Sodium metal chip (99.7%, AOT battery). Sodium bis(fluorosulfonyl)imide : N-Methyl-N-propylpyrrolidinium bis(fluorosulfonyl)imide (1:9 mol ratio) (NaFSI:PYR_{13}FSI, 99.9%, Solvionic).

1. Preparation of oriented porous NASICON scaffolds and reference NATP disc solid electrolyte

Commercial sodium aluminum titanium phosphate ($Na_{1.3}Al_{0.3}Ti_{1.7}P_3O_{12,}$ NATP) powder was obtained from NEI Corporation, USA. The NATP powder (1 g) was ball-milled at 300 rpm for 3 hours using planetary ball mill (Pulverisette 7PL, Fritsch), in ZrO_2 jars (20 mL) with 10 ZrO_2 balls (5 mm in diameter). Subsequently, the ball-milled powder was dispersed in 20 ml isopropanol and sonicated for 4 hours in ultrasonic bath to break up agglomerated particles. The resulting mixture was then dried at 80 ^oC in vacuum oven and then used for the freeze-casting experiments.

To prepare the slurry for freeze casting process (**Scheme 1**), an aqueous solution (2 ml) of 10 wt. % polyvinyl alcohol was first prepared. The NATP powder (400 mg) was then dispersed in the solution and polyethylene glycol (18 µl) was added as a plasticizer. The solution was sonicated for one hour in an ultrasonic bath and then stirred overnight at 300 rpm to obtain homogenous slurry for the freeze-casting process. The freeze casting process was then carried out in an in-house setup comprising of a copper cold finger. The slurry (~300 µl per sample) was poured into in-house made PTFE mold (inner diameter 17 mm and 2 mm thickness with metallic base) and upon freezing on top of the copper cold finger, it was immediately transferred to a lyophilizer to sublime the ice. The freeze-cast sample thus obtained was then sintered at 900 ^{o}C in air for 6 hours to obtain the oriented porous NATP solid electrolyte scaffold.

The reference NATP disc solid electrolyte was prepared by pelletizing 200 mg of NATP powder in a Ø13 mm die set at a load of 2 tons for 5 minutes with a hydraulic press. The green pellet was then sintered at 900 ^{o}C in air for 6 hours to obtain the NATP disc solid electrolyte.

2. Synthesis of $Na_3V_2(PO_4)_3$ cathode (NVP) active material

The cathode material $Na_3V_2(PO_4)_3$ was synthesized according to a previous report.[1] Briefly, an aqueous suspension was formed by adding 4 mmol of vanadium pentoxide (V_2O_5), 12 mmol of ammonium dihydrogen phosphate ($NH_4H_2PO_4$), and 6 mmol of sodium carbonate (Na_2CO_3) into 35 mL of distilled water and stirring the mixture at room temperature. 6 mmol of ascorbic acid and 3 mL of polyethylene glycol were then added to the mixture. The resulting blue suspension was stirred for 30 minutes before being transferred to a 45 mL Teflon-lined autoclave (Parr Instrument Company). The sealed autoclave was kept at 180 ^{o}C for 40 hours and then cooled to room temperature. The resulting brown mixture was ultrasonically treated for 90 minutes to create a uniform dispersion, and then heated on a hot plate at 95 ^{o}C with stirring to evaporate water. The obtained brown sol was dried at 120 ^{o}C overnight. The

precursor was then ground and preheated at 350 ^{o}C for 4 hours. Finally, the preheated sample was ground to powders and calcined at 750 ^{o}C for 6 hours in a flowing argon atmosphere.

3. Cathode material infiltrated NATP scaffolds and electrochemical characterization

A slurry was prepared by mixing 80 wt.% NVP, 10 wt.% carbon black, 10 wt.% polyvinylidene fluoride in *N*-methyl-2-pyrrolidone (NMP). For preliminary half-cell studies of the cathode, the slurry was coated on a carbon-coated aluminum foil using a doctor blade (150 µm) and dried under vacuum at 100 ^{o}C overnight. Circular electrodes (Ø11 mm) were punched and assembled into CR2032 coin cells with glass microfiber separator soaked in 1M $NaClO_4$ in propylene carbonate (PC) and 5% fluoroethylene carbonate (FEC) electrolyte and Na metal chip as the counter electrode.

For cathode material infiltration, the slurry was drop-cast onto the NATP scaffolds. The samples were placed in a vacuum oven at 100 ^{o}C overnight to obtain the cathode infiltrated NATP scaffolds. The composite structures were then assembled into coin cells inside an argon-filled glove box. To reduce the interfacial resistance, 20 µl of ionic liquid electrolyte NaFSI:PYR_{13}FSI was added on the cathode infiltrated side and the Na metal chip was used as the anode. 10 µl of the ionic liquid was added at the Na/FC-NATP interface. The coin cells were subjected to galvanostatic cycling using a Biologic VMP3 multichannel potentiostat/galvanostat. The cycling was carried out in the potential window 2-4 V at different specific currents of 50-200 mA $g^{-1}_{cathode}$ after 12 hours of rest. The electrochemical impedance spectroscopy was carried out in a Biologic SP200 potentiostat/galvanostat equipped with a frequency response analyzer in the frequency range 7 MHz-100 mHz. For plating and stripping studies, the NATP scaffolds were sandwiched between sodium metal chips and different currents (± 50-1000 µA cm^{-2}) were applied for 1h Na plating and stripping steps.

4. Material Characterization

X-ray diffraction (XRD) patterns were obtained using a PANalytical Empyrean powder diffractometer in reflection mode with Cu Kα radiation (45 kV, 40 mA). Scanning electron microscopy (SEM) analyses were conducted using a Carl Zeiss GEMINI SEM 450. Prior to analysis, the samples were sputtered with a 6 nm thick layer of platinum. Thermogravimetric analyses were performed using a Mettler Toledo TGA/SDTA 851e instrument under atmospheric air conditions with a flow rate of 50 mL/min and a heating rate of 10°C/min.

X-ray computed tomography and porosity calculation: Micro-CT analysis was performed using an EasyTom XL Ultra 230-160 micro/nano-CT scanner (RX Solutions, Chavanod, France). The scanner was set to an X-ray source voltage of 90 kV and a current of 160 µA. The samples were scanned over a full 360° with a rotation step of 0.2° and a frame average of 10. The nominal resolution was set to 700 nm voxel size. The scans were reconstructed into 16-bit TIFF format cross-section images using the scanner reconstruction software. For measurements and quantification, a cubic volume of interest (VOI) of 0.5 mm side was selected within the sample. Channel quantification was performed by segmenting the tomographic slices of the VOI using the Otsu thresholding algorithm with the image analysis software Avizo (Thermo Fisher Scientific, USA), and porosity was calculated as a percentage of the bulk volume of the sample.

Scanning Transmission Electron Microscopy imaging: The NATP powder was dispersed in methanol and drop-cast onto a regular copper TEM-grid covered with a lacey carbon support film. The sample was cleaned in an Ar-O plasma for two rounds of 3 seconds before being inserted into the microscope. High-angle annular dark-field scanning transmission electron microscopy (HAADF-STEM) images and energy-dispersive X-ray spectroscopy (EDX)

elemental maps were acquired with a probe-corrected Titan Themis operated at 300 kV. The EDX maps were recorded with the Super-X detector system from Thermo Fisher.

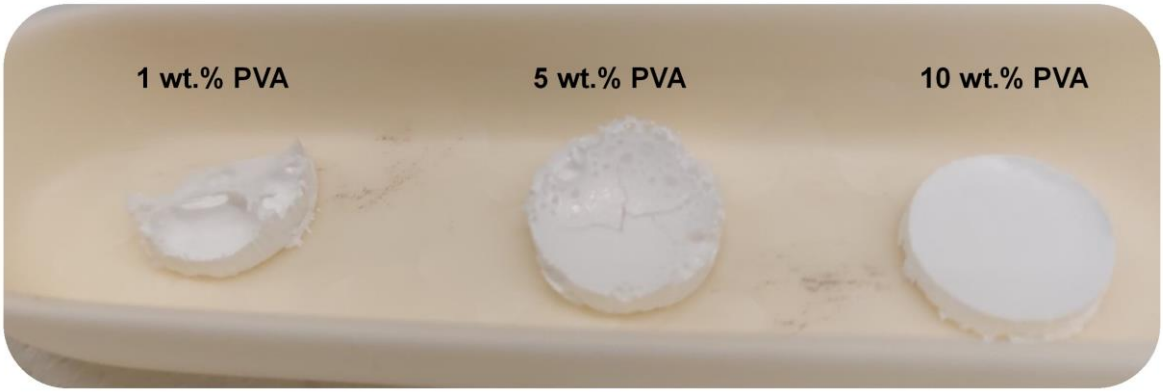

Figure S1. Photographs of freeze-cast NATP pellets with different weight ratios of PVA binder (before sintering).

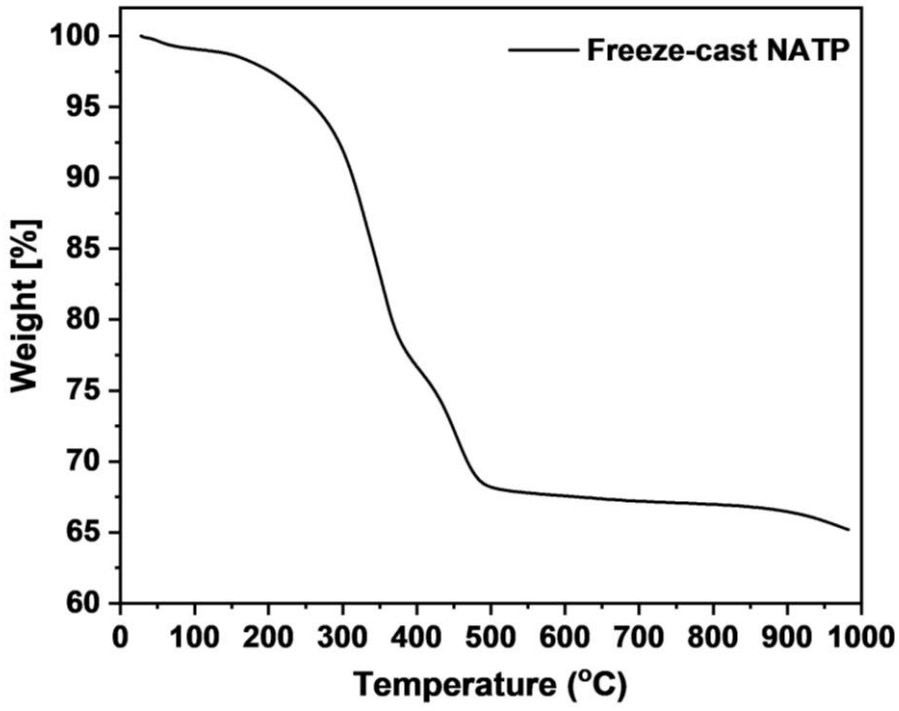

Figure S2. Thermogravimetric analysis of freeze-cast NATP sample.

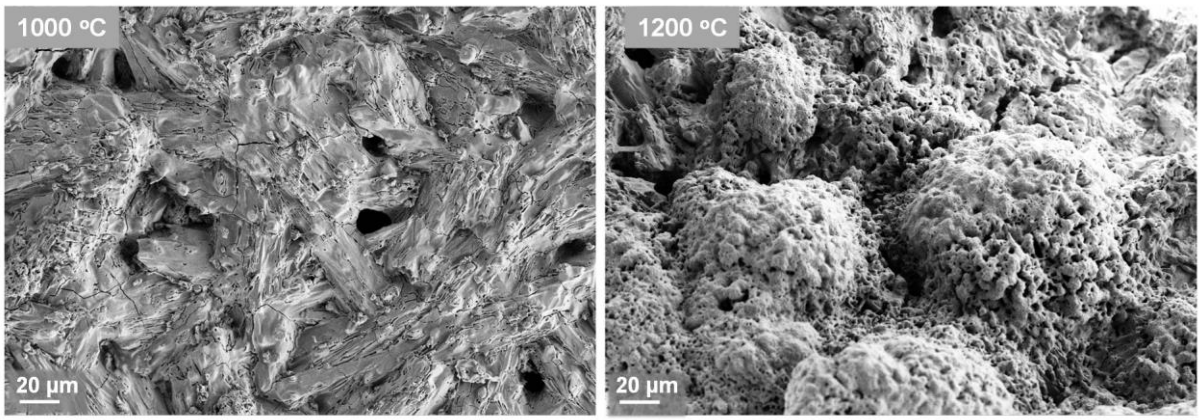

Figure S3. SEM images of freeze-cast NATP sample after sintering at 1000 and 1200 °C.

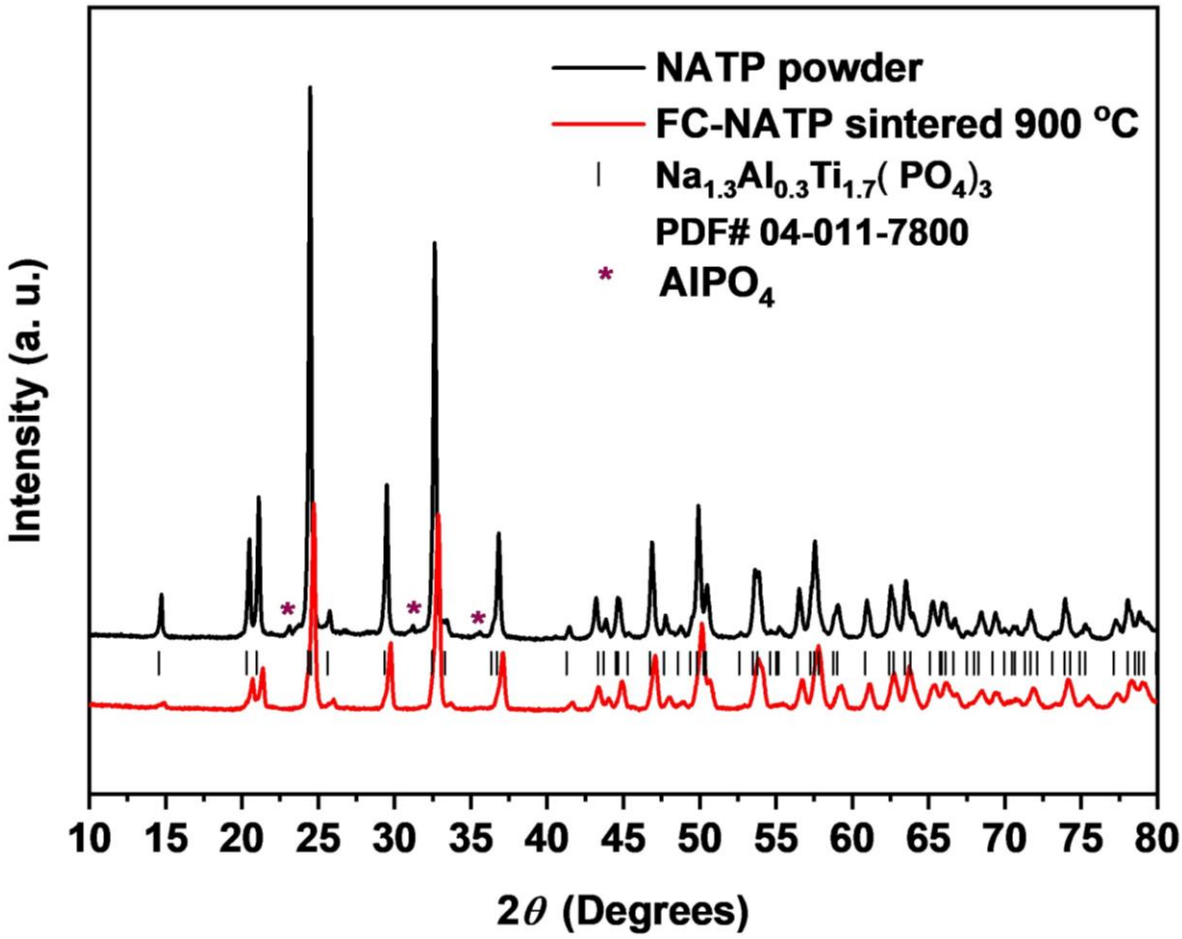

Figure S4. X-ray diffractogram of freeze-cast NATP before and after sintering at 900 °C together with the reference pattern as vertical bars.

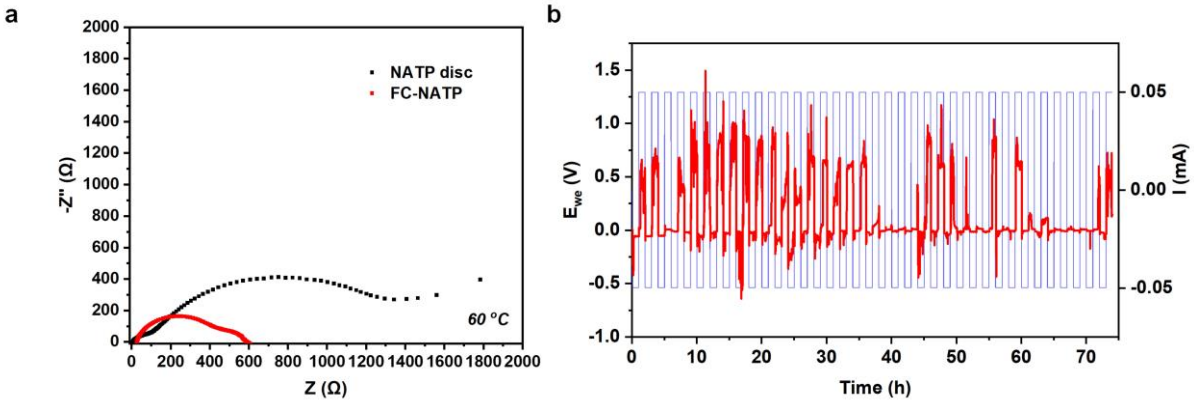

Figure S5. a) Electrochemical impedance spectra of symmetric sodium cells Na|| NATP disc||Na and Na||FC-NATP||Na at 60 ^{o}C. b) Plating and stripping performance of Na||NATP disc||Na cell at current density of 50 µA cm^{-2}. ~10 µl of the ionic liquid was added at the Na||NATP and Na||FC-NATP interfaces.

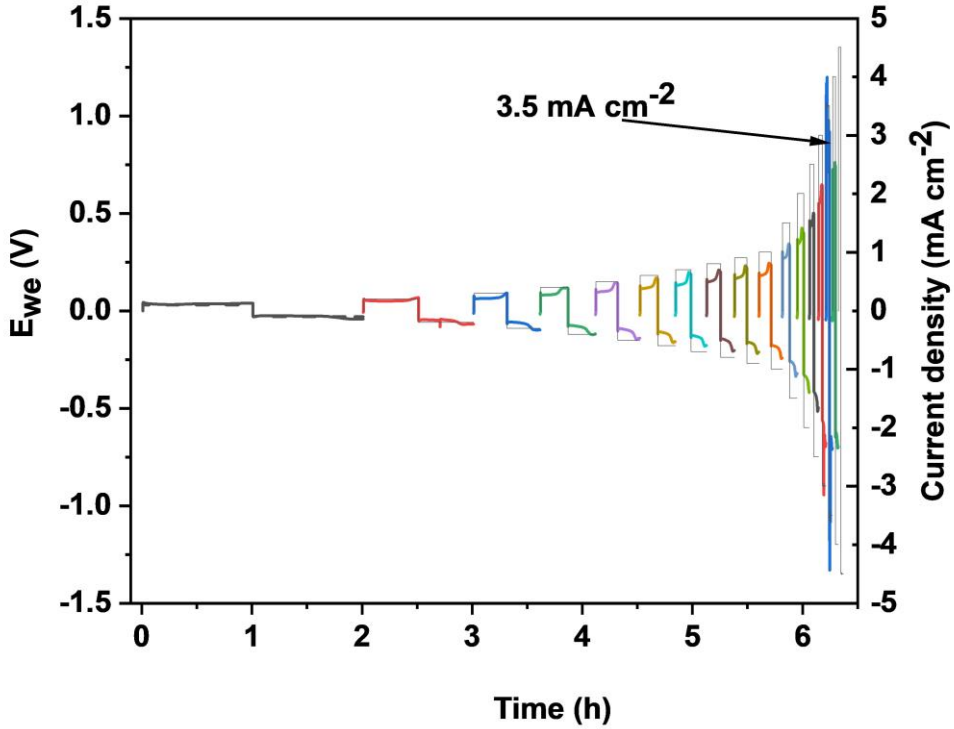

Figure S6. Critical current density measurements of Na||FC-NATP||Na symmetric cells at 60 ^{o}C conducted with a capacity limitation of 0.1 mAh cm^{-2} per half-cycle. ~10 µl of the ionic liquid was added at the Na||FC-NATP interfaces.

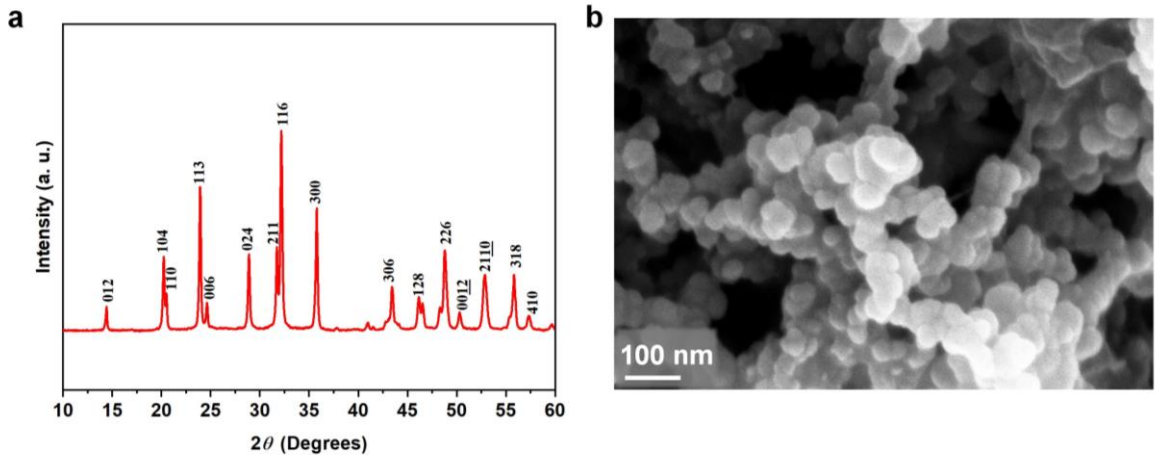

Figure S7. a) XRD pattern and b) electron microscopy image of the synthesized NVP nanoparticles.

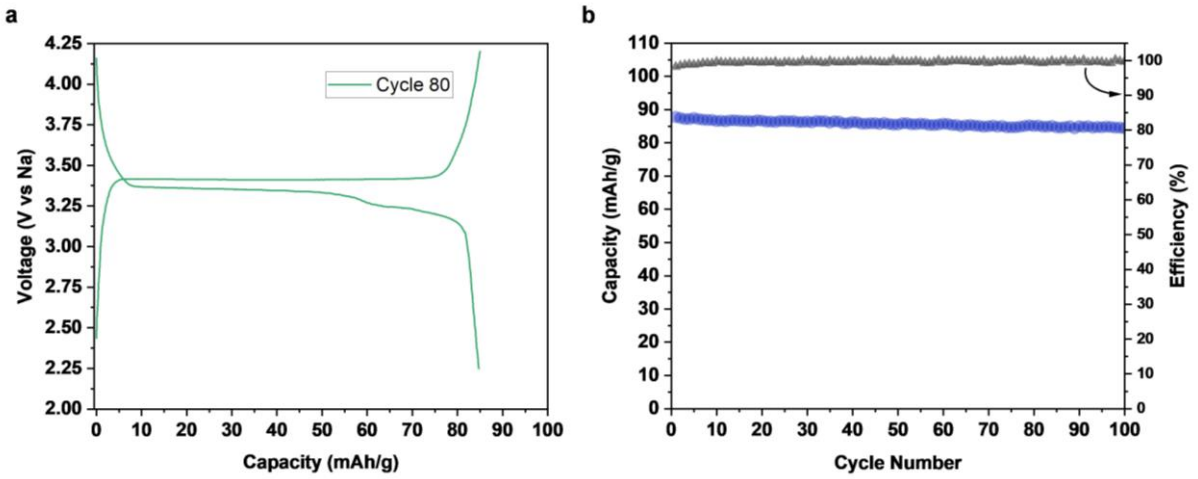

Figure S8. a) Potential profile and b) galvanostatic cycling performance of the NVP cathode in Na half-cell with liquid electrolyte (1M $NaClO_4$ in propylene carbonate and 5 vol.% fluoroethylene carbonate) at a specific current of 50 mA g^{-1}.

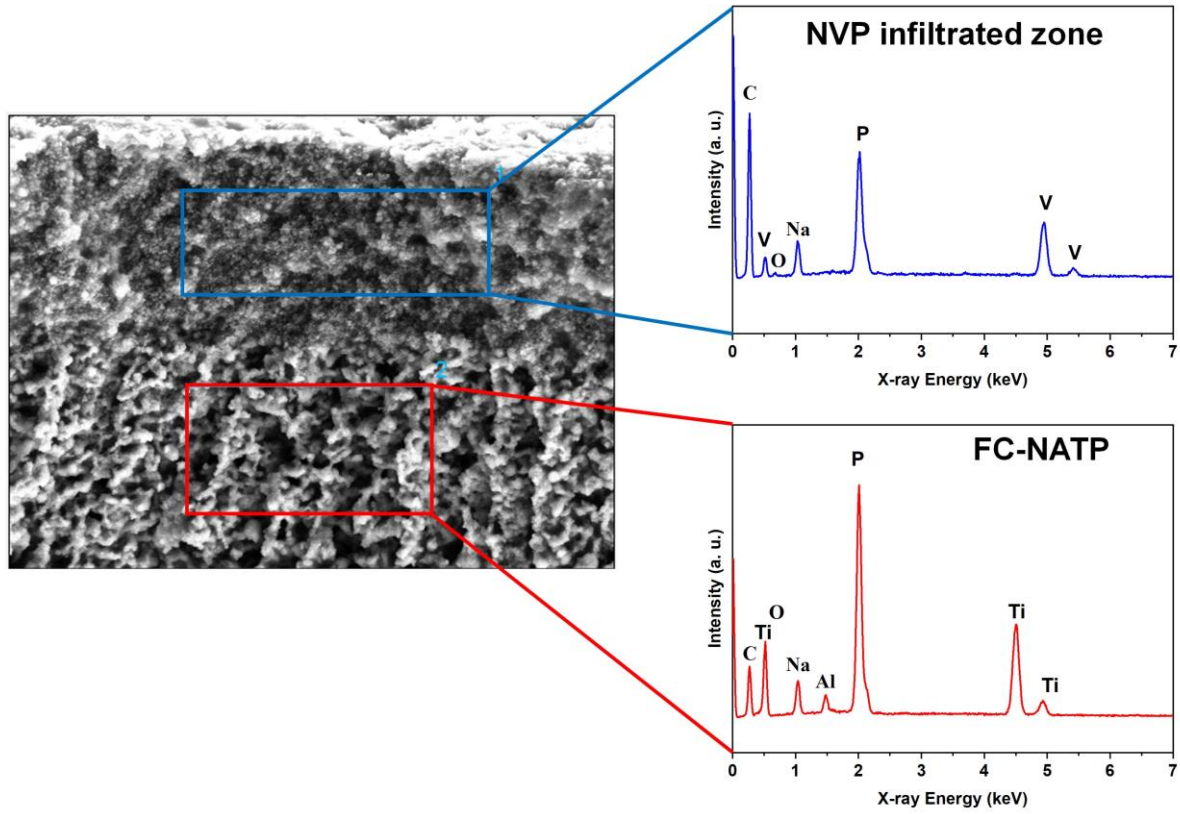

Figure S9. EDX elemental spectra of the NVP infiltrated and the FC-NATP zones in NVP_FC-NATP.

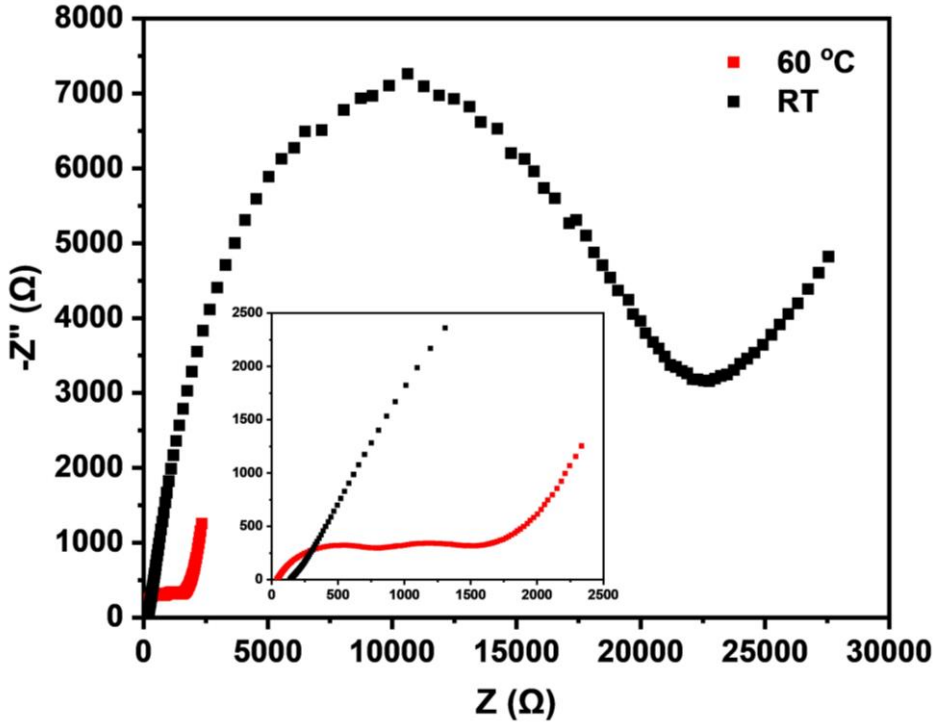

Figure S10. Electrochemical impedance spectra of NVP_FC-NATP||Na cell without ionic liquid.

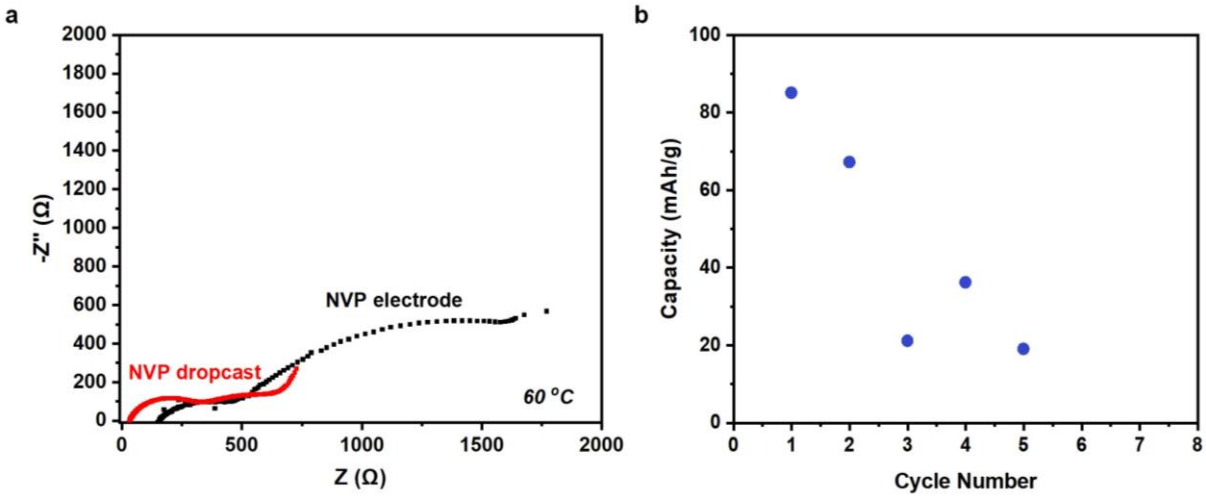

Figure S11. a) Electrochemical impedance spectra of NVP_FC-NATP||Na (NVP dropcast) and $NVP_{electrode}$||NATP||Na cells (NVP electrode) with ionic liquid at interfaces. b) Galvanostatic cycling performance of $NVP_{electrode}$||NATP||Na cell at 50 mA g^{-1}.

Table S1 Comparison of electrochemical performance of as-developed NVP_FC-NATP||Na cell with recently reported sodium metal batteries.

Electrodes	**Electrolyte**	**Testing temperature**	**Capacity (mAh g^{-1}) (current rate)**	**Cycle number**	**Capacity retention**	**Mass loading, mg cm^{-2} (current density, mA cm^{-2})**	**Ref**
$Na_3V_2PO_4$||Na	Freeze-cast $Na_{1.3}Al_{0.3}Ti_{1.7}P_3O_{12}$ (NATP)	60 °C	93.8 (50 mA g^{-1})	100	94%	3 (1)	This work
$Na_3V_2PO_4$||Na	$Na_3Zr_2Si_2PO_{12}$	80 °C	104.5 (11.7 mA g^{-1})	120	91%	2.5 (0.1)	2
$Na_3V_2PO_4$||Na	β″-Al_2O_3	60 °C	87 mAh g^{-1} (11.7 mA g^{-1})	100	95.5%	6.5 (0.07)	3
$Na_2MnFe(CN)_6$||Na	$Na_3Zr_2Si_2PO_{12}$-PEO-$NaClO_4$	60 °C	109 (85.5 mA g^{-1})	300	83%	3 (1)	4
Na_xCoO_2||Na	$Na_{3.4}Sc_{0.4}Zr_{1.6}(SiO_4)_2(PO_4)$	RT	142 (0.15C)	100	75%	0.4 (8 μA cm^{-2})	5
Mo_6S_8||Na-Sn	Na_3PS_4	60 °C	75 (60 mA g^{-1})	500	69%	2 (0.01)	6
$NaCu_{1/9}Ni_{2/9}Fe_{1/3}Mn_{1/3}O_2$||Na	NaFNFSI/PEO	80 °C	105 (120 mA g^{-1})	150	70%	1.8 (0.1)	7

References

(1) Duan, W.; Zhu, Z.; Li, H.; Hu, Z.; Zhang, K.; Cheng, F.; Chen, J. Na3V2(PO4)3@C Core–Shell Nanocomposites for Rechargeable Sodium-Ion Batteries. J. Mater. Chem. A 2014, 2, 8668-8675.

(2) Zhang, Z.; Wenzel, S.; Zhu, Y.; Sann, J.; Shen, L.; Yang, J.; Yao, X.; Hu, Y.-S.; Wolverton, C.; Li, H.; Chen, L.; Janek, J. Na3Zr2Si2PO12: A Stable Na+-Ion Solid Electrolyte for Solid-State Batteries. ACS Appl. Energy Mater. 2020, 3, 7427-7437.

(3) Lai, H.; Li, Y.; Wang, J.; Li, W.; Wu, X.; Wen, Z. Design of Solid-State Sodium-Ion Batteries with High Mass-Loading Cathode By Porous-Dense Bilayer Electrolyte. J. Materiomics 2021, 7, 1352-1357.

(4) Yu, X.; Xue, L.; Goodenough, J. B.; Manthiram, A. A High-Performance All-Solid-State Sodium Battery with a Poly(ethylene oxide)–Na3Zr2Si2PO12 Composite Electrolyte. ACS Mater. Lett. 2019, 1, 132-138.

(5) Kehne, P.; Guhl, C.; Ma, Q.; Tietz, F.; Alff, L.; Hausbrand, R.; Komissinskiy, P. Sc-Substituted NASICON Solid Electrolyte for an All-Solid-State NaxCoO2/NASICON/Na Sodium Model Battery with Stable Electrochemical Performance. J. Power Sources 2019, 409, 86-93.

(6) Yue, J.; Zhu, X.; Han, F.; Fan, X.; Wang, L.; Yang, J.; Wang, C. Long Cycle Life All-Solid-State Sodium Ion Battery. ACS Appl. Mater. Interfaces 2018, 10, 39645-39650.

(7) Ma, Q.; Liu, J.; Qi, X.; Rong, X.; Shao, Y.; Feng, W.; Nie, J.; Hu, Y.-S.; Li, H.; Huang, X.; Chen, L.; Zhou, Z. A New Na[(FSO2)(n-C4F9SO2)N]-Based Polymer Electrolyte for Solid-State Sodium Batteries. J. Mater. Chem. A 2017, 5, 7738-7743.